VOL. 13, NO. 6, MARCH 2018 ISSN 1819-6608
ARPN Journal of Engineering and Applied Sciences

www.arpnjournals.com

FAULT LINEAMENTS AND DEPTH ESTIMATION BY AEROMAGNETIC DATA OF MERSING FAULT ZONE IN JOHORE, PENINSULAR MALAYSIA

Nurul Fairuz Diyana Binti Bahrudin and Umar Hamzah
Geology Programme, School of Environmental and Natural Resource Sciences, Faculty of Science and Technology, Universiti Kebangsaan Malaysia, Bangi, Selangor, Malaysia
E-Mail: nurulfairuz@nuclearmalaysia.gov.my

ABSTRACT

Aeromagnetic data covering an area of 1800km^2 were analysed to characterise the dimension of Mersing fault zone and the surrounding faults by conventional processing including filtering and 3D Euler Deconvolution techniques using Oasis Montaj computer software. Based on the analysis, the position of the Mersing fault zone including its trend, width and sense of displacement were clearly determined and comparable with the geological input of previous findings. New inputs from this study are derived from 3D Euler Deconvolution in terms of the subsurface geometrical position of major and minor faults in the study area including dip and depth parameters.

Keywords: structural lineaments, mersing fault, peninsular Malaysia, oasis montaj software, 3D euler deconvolution.

INTRODUCTION

Magnetics values from the available aeromagnetic maps of Agocs and Paton (1966) were digitized and reprocessed using Surfer and Oasis Montaj software in an attempt to reinterpret the Mersing fault zone in terms of its position and depth. Samsudin *et al.* (2000) had studied and processed the same data and arrived in determining several linear features associated with concentrating of magnetic minerals along fault zone. Corresponding to the major tectonic fault system of Peninsular Malaysia.

Mersing fault zone is considered as part of major fault zones in Peninsular Malaysia as reported by Hutchinson *et al.* (2009). Tjia (1972) described the fault zone as having a strike along 290^{0}E-300^0 E and considered to be a dextral strike-slip fault width about 20-20km shift. Tjia (1977) identified the Mersing fault zone as an eastern extension of Kuala Lumpur fault zone which was most likely originated during the end of tectonic activity in late Cretaceous. Similar age of the fault was also confirmed by Chong *et al.* (1968). All these information only described the surface features of the Mersing fault as derived from geological information as well as magnetic studies. None has been reported on the subsurface properties of the faults including its subsurface extension and the depth of the fault into the basement.

This studies attempt to estimate the dip and depth extend of the fault zone based on 3D magnetic Euler Deconvolution. This technique has successfully been used by Gopal K.G (2016) in interpreting the tectonic features such as thrusting and faulting in the North-West and North-East of Himalaya. In his study, various thrust and fault locations were nicely super imposed with Euler source depth solutions. Ghosh (2013) managed to estimate the some depth by the same technique representing positions of faults/thrusts within the basement at depth estimation of about 5-12km. Not only the Euler source depth points formed lineaments that overlapped with the existing faults and thrusts zones, but the new and non-overlapped lineaments also can be used to estimate as indication of new faults and thrust zones.

The study area is located in Johore within 102.96^{0}E-103.53^{0}E longitude and 2.41^{0}N-2.67^{0}N latitude covering an area of 1800km^2(Figure-1). In this study attempts have been made to estimate the areal and depth extent of the fault zone especially its dipping direction which has not been reported by previous researchers.

METHODOLOGY

Magnetic and gravity surveys are well known potential field techniques widely used in oil, minerals and geological faults exploration. In this study a total of about 35380 magnetic field data were digitized from aeromagnetic maps using surfer computer software (Agocs & Paton 1966). The aeromagnetic map of Mersing fault zone was digitized and reinterpreted by Oasis Montaj software. The digitized data were converted from Latitude-longitude positions into a Universal Transverse system before they can be processed by Oasis Montaj software. These aeromagnetic data were already processed to produce a reduce-to-equator (RTE) map and later being used in filtering packages for deriving the total horizontal derivatives (THD), total vertical derivatives (TVD) and Euler deconvolution.

According to Cooper & Cowan (2008), edge enhancement by TVD and THD filtering techniques very much helps in geological interpretation especially in fault and lineaments characterization. THD is calculated by a formula given below;

$$THD = \sqrt{\left[\frac{df}{dx}\right]^2 + \left[\frac{df}{dy}\right]^2} \quad (1)$$

where f is the magnetic field in x and y direction (Cordell and Grauch, 1985). THD derivative filtering technique was used to estimate the linear structures such as faults and contacts from the potential data (El-Khafeef and El Khodary, 2011). Vertical derivative filtering

technique (TVD) was used to estimate the width of source bodies or anomalies more precisely (Thurston and Smith, 1997) and the value is calculated by formula given below; where *f* is the magnetic field in z direction.

$$TVD = \sqrt{\left[\frac{df}{dz}\right]^2} \quad (2)$$

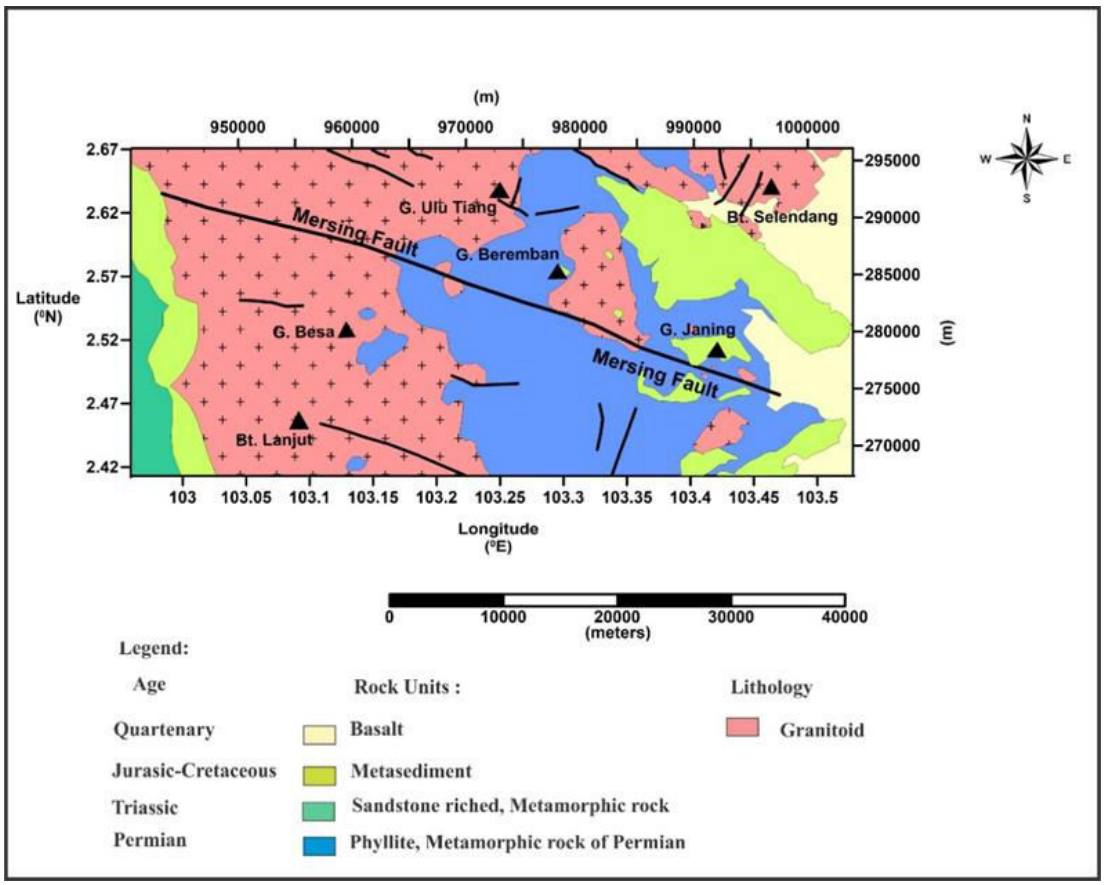

Figure-1. Geological map of Mersing fault zone (MGD, 2014).

Amigun *et al.* (2012) used Euler deconvolution technique to locate the iron ore bodies and their depths in Okene, Nigeria. Euler deconvolution technique was also used to locate the point source of anomaly and its depth as reported by Reid *et al.*, (1990). The technique was used and applied to the gridded or profile data to solve the Euler's homogeneity equation (Thompson, 1982). The 3D Euler deconvolution is defined by the equation given below, where x_0, y_0 and z_0 are the source locations; F is the magnetic field measured at *x, y, z* points; B is the total field value; N is the Euler's Structural Index (SI) which characterizes the source geometry (Reid, 1997).

$$(x - x_0)\frac{dF}{dx} + (y - y_0)\frac{dF}{dy} + (z - z_0)\frac{dF}{dz} = -N(B - f) \quad (3)$$

RESULTS AND DISCUSSIONS

The reduced to equator map (RTE) map shows the total magnetic anomalies are ranging from 2054 to 2309 nT (Figure-2). Faults positions as deduced by previous geological studies were also drawn on the same map. Magnetic lineaments were interpreted from the RTE map along boundaries of magnetic highs and lows. Based on the picked lineaments, major and minor interpreted faults trends are in N115^{0}E which is equivalent to WNW-ESE. This trend is also observed using radar-sat as stated in Hutchison and Tan (2009). This fault direction is also quite similar to the Kuala Lumpur fault therefore the Mersing fault zone can also be interpreted as a possible continuation of the Kuala Lumpur fault zone to the east (Stauffer, 1968).

Based on RTE map and the high magnetization band in the south of the study area, the width of the fault zone can be estimated as approximately 20km which is smaller than estimated by Stauffer (1968). Another major lineament direction observed in the RTE map is trending along N80^{0}E. The major fault trend of NW-SE direction is comparable with the radar-sat finding which is almost E-W in direction. The high magnetic values along the faults are due to magnetic minerals within the fault zone extending into the basement. Basically, it can be concluded that faults determine based on high magnetization are not much in difference with those determined by radar-sat since radar-sat lineaments are based on physical faults position and high magnetization is also found in fault zone. Based on these two major faults trend, the displacement of crustal material along the faults can be estimated to be a left lateral type where the sense of

movement is indicated by the NW-SE faults in the northern part of Mersing fault. This NW-SE shorter lineament length between 5 to 15km are clearly represented by high magnetization stripes in the RTE map (Figure-2). This left lateral displacement was also observed by Tjia (1972, 1977); Syed Sheikh Almashoor (1989). The trend of WNW-ESE to NW-SE fault are similar to that of the Kuala Lumpur fault zone indicating similar fault age of post Upper Triassic Main Rain Granite intrusion as reported by Hutchinson and Tan (2009).

THD and TVD filtering techniques are often used in potential field data processing for gravity and magnetic especially for determining details edges or lineaments. These technique were used in this study for estimating potential structure features such as faults and joints. THD map produced is shown in Figure-3 indicating magnetic patterns with values ranging from $1x^{10-4}$-$10.11x10^{-2}$nT. In general, the THD map indicates the presence of straight and curve short lineaments or edges associated with high magnetic anomalies. Each lineament has been selected and noted as dashed lines and interpreted as faults with length ranging from 2 to 15km along major trend of NW-SE, NNE-WSW and minor trend of E-W and ENE-WSW in direction. The minor trend fault direction of ENE-WSW found in the northern part of Mersing fault zone can be an indicator of left lateral displacement along the Mersing fault zone. The fault lineament determined by the MGD (2014) also equivalent to lineament observed by THD map as also shown in Figure-3.

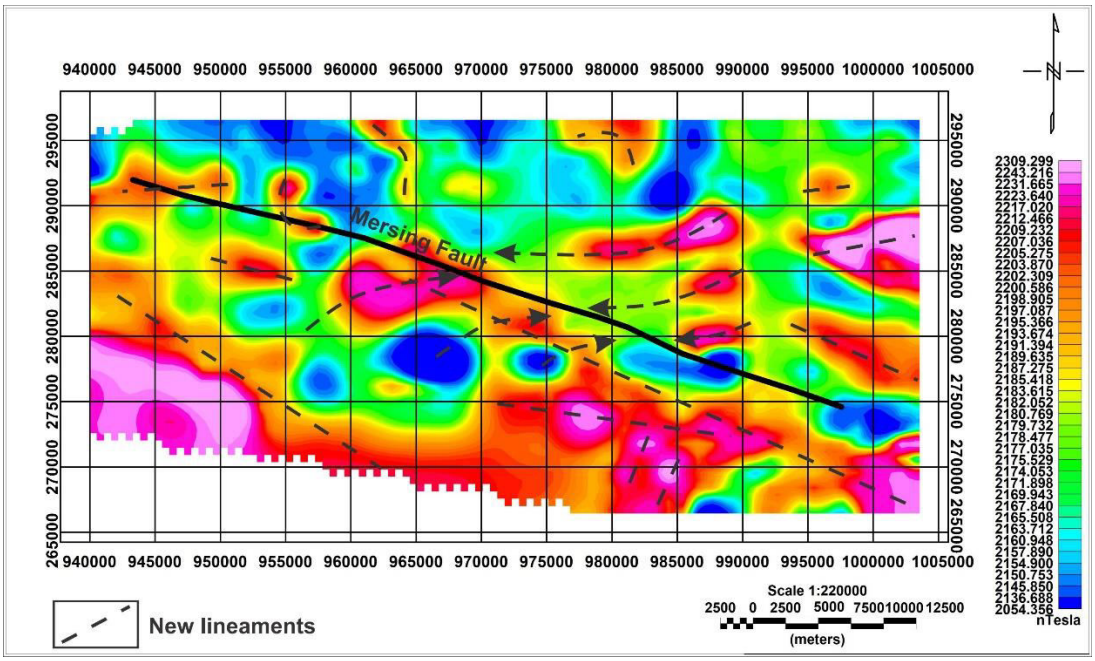

Figure-2. Reduce to the equator magnetic anomaly map.

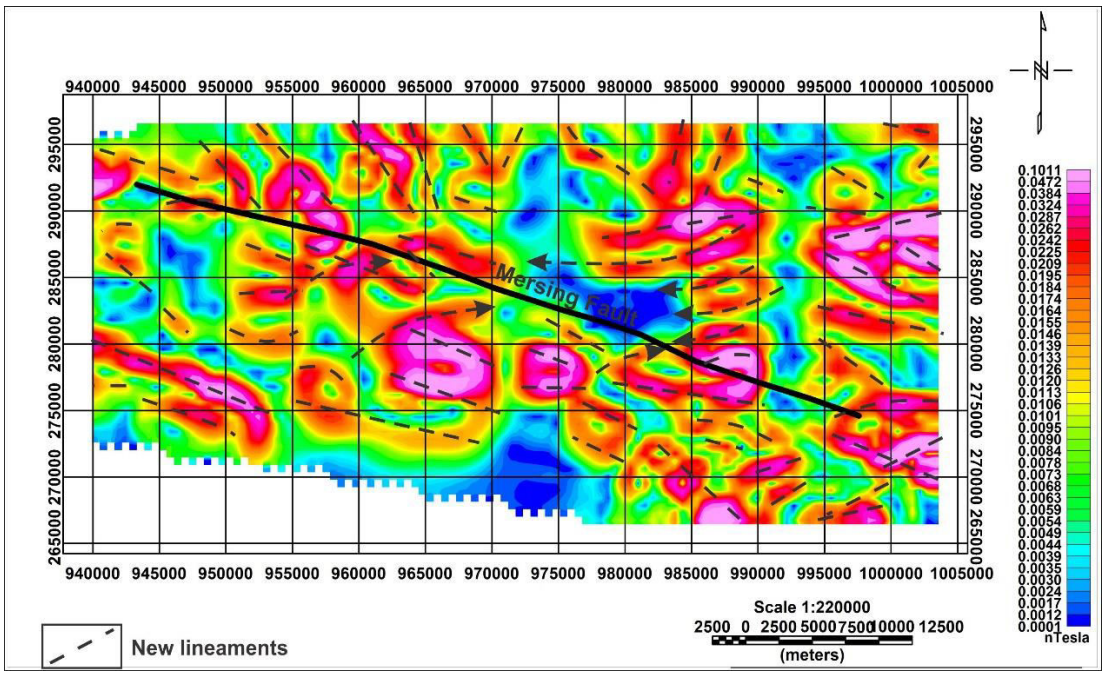

Figure-3. Total horizontal derivative (THD) map.

Figure-4 shows the vertical derivatives (TVD) map which represent highs and lows of vertical magnetic component values. The map highlighted the distribution many straight and curve features with length ranging from 1 to 20km and magnetic values of $2.6x10^{-3}$to $123.1x10^{-4}$ nT. The patterns of magnetic lineament are much simpler compared to THD lineament patterns. Accordingly the short lineaments were selected and drawn as dashed lines representing potential faults. The selected lineaments fall along dominantly NW-SE especially in the southern part of Mersing fault zone. While other few E-W, E-NE and W-SW lineaments are found in the northern part of the Mersing fault zone. Similar sinistral strike-slip faults can be deduced from this faults trend.

The RTE data was also inversed to produce Euler anomaly point sources distribution using structural index (S.I) value of 0.5 and window (W) size of 5. These SI and W factors were arrived by trial and error techniques. Euler maps that produced numerous lineaments similar to fault patterns are considered as the more suitable SI and W factors. According to Reid (2014), SI value of 0.5 is used for estimating fault and finite contacts. Window scale 5 is used as determining the size of grid data input of about 5 x 5 km^2. Figure-5 shows the distribution of Euler anomaly point sources with various depth ranging from 0.2 to 6km covering the whole study area in the vicinity of Mersing fault zone.

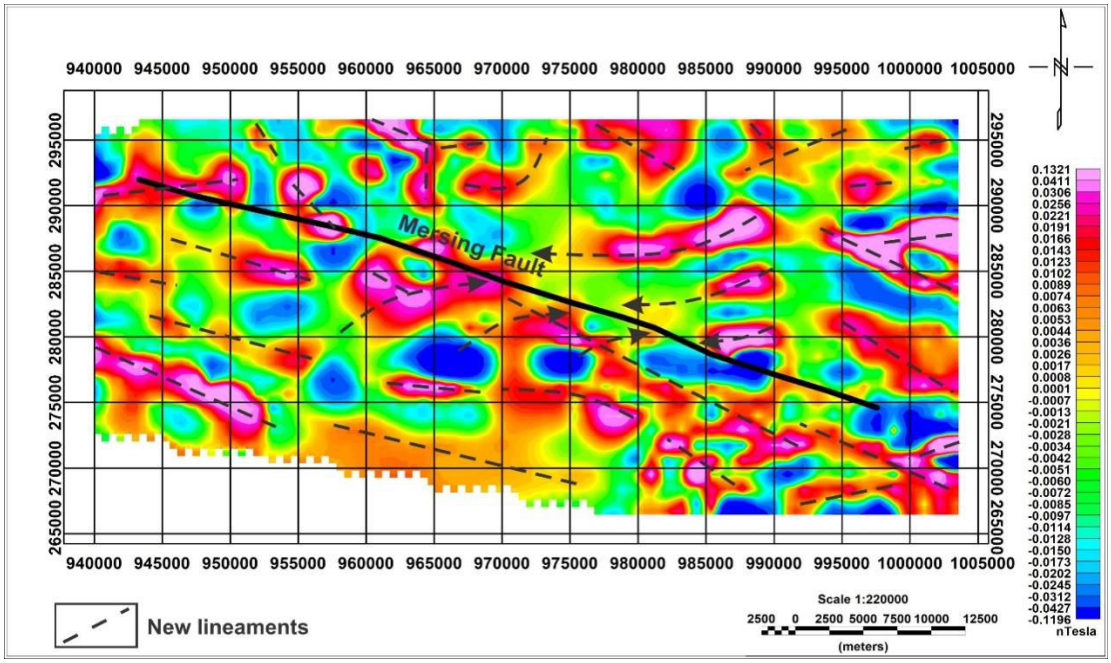

Figure-4. Total vertical derivative (TVD) map.

The Euler point source map clearly shows the distribution of anomaly point source along straight line patterns which can be associated with source of anomaly along faults and joints with length of about half to 20km. Figure-5 also shows position of Mersing fault zone and smaller faults surrounding it as determined by geological map of Peninsular Malaysia (MGD, 2014). All points along straight lines and curves are joined to produce lineament features with length from half to 20km as shown in Figure-6. All trends of Euler possible lineaments are considered as fault strike position and this strike were measured and plotted in rose diagram as well as histogram. Based on rose diagram (Figure-6b) and histogram (Figure-6c), the most dominant fault strike is E-W in direction, followed by WNW-ESE, NNW-SSE and finally SSW-NNW. Most of these lineaments observed in the Euler map indicate source depth of fault ranging from 1 to 2km with a few 3 to 4km. These faults are originated within the crustal material in phyllitic metasediment to Cretaceous metasediment as well as in granitoids. The sense of sinistral strike-slip fault movement is more profound in the interpreted Euler map (Figure-6a) whereby the northern block movement to the northwest is indicated by the ENE-WSW and NE-SW faults in the northern part of Mersing fault zone as indicated by arrows.

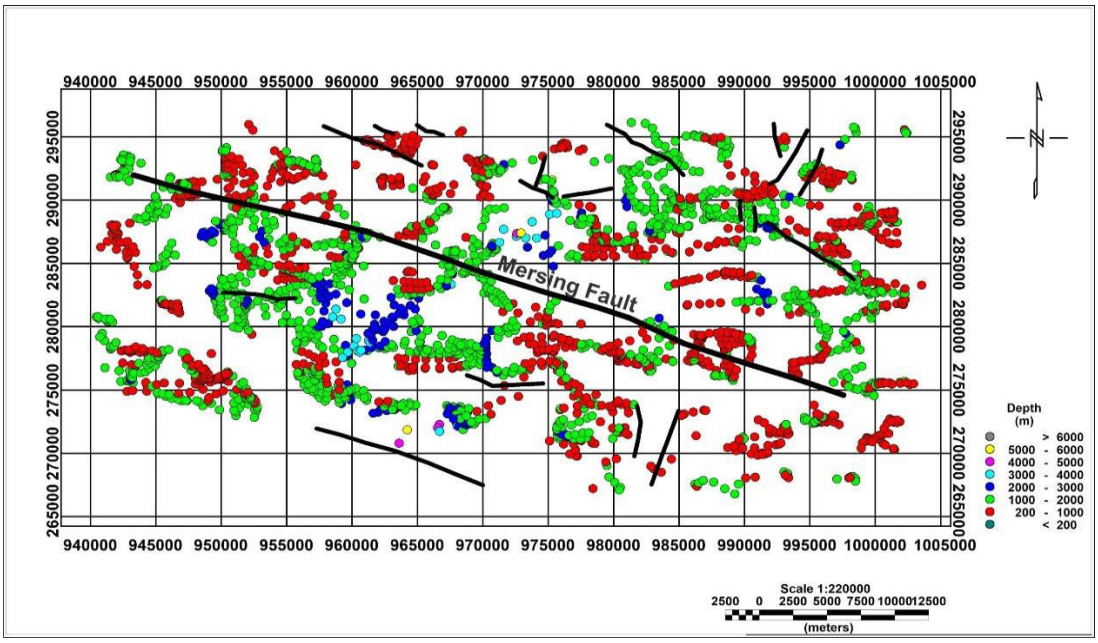

Figure-5. Euler anomaly pointsource map with SI 0.5 and W 5 was overlapped with the existing fault lines.

ISSN 1819-6608
ARPN Journal of Engineering and Applied Sciences

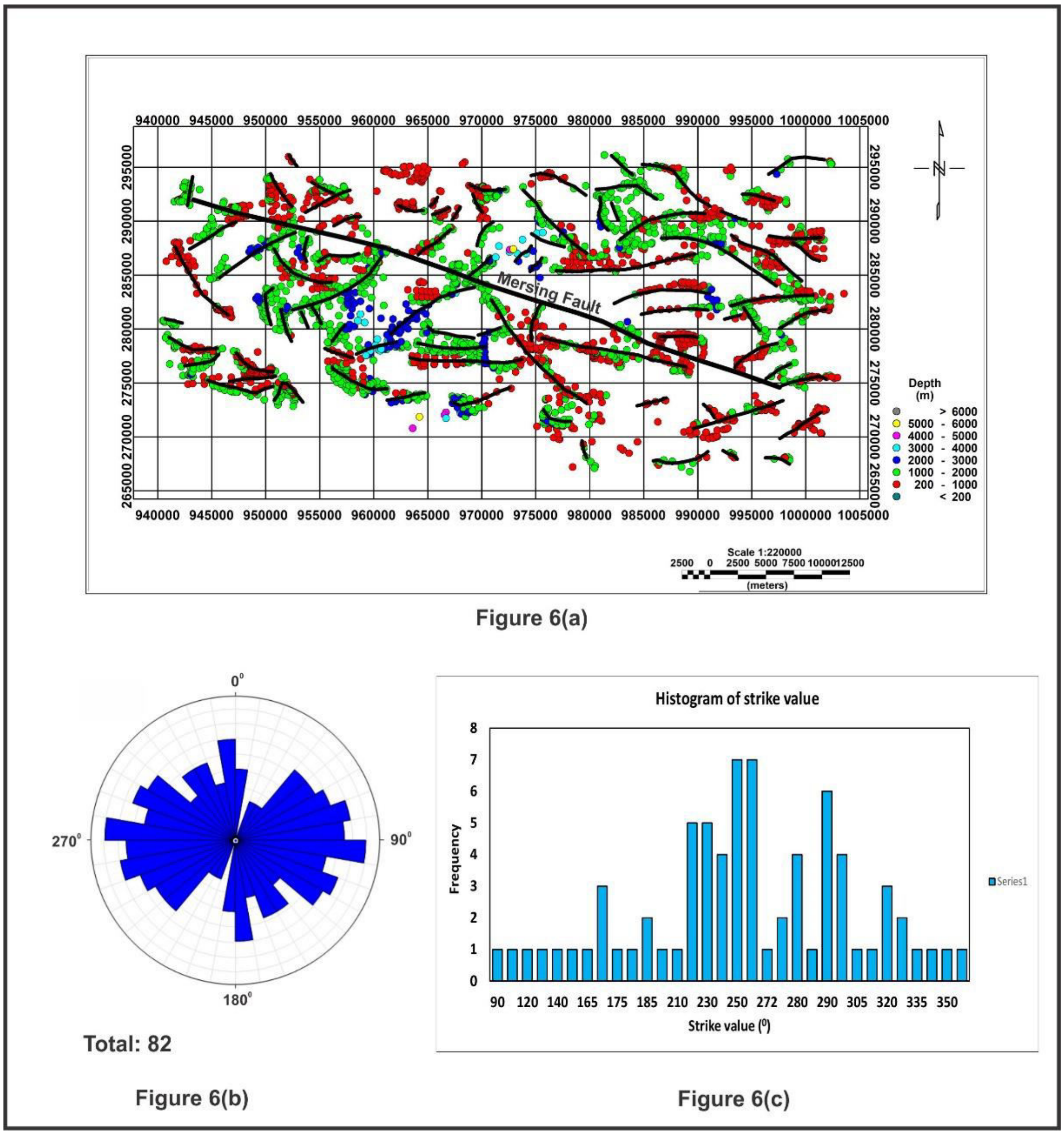

Figure-6(a). Euler anomaly point source map with fault interpretation.
Figure-6(b). Rose diagram of selected faults.
Figure-6(c). Histogram of the fault strikes.

A corridor along east-west between 2.51^0N to 2.57^0N latitude (Figure-7a) was chosen for generating Euler point source depth cross-section purposely for determining possible fault dips and depths below the surface. Figure-7b indicates the Euler subsurface cross-section indicating the possible faults location along the E-W. Most of the point source depth from surface to about 3km falls along simple straight lines dipping in various directions. There were some points scattered within the Mersing fault zone at 35 to 40 km from the western border. The dips and maximum depths of each fault were calculated and shown in Table-1. The fault dips range from $12^0$to 89^0. The strike directions of these faults were determined by recognizing the faults on the Euler map along the corridor. The fault strike direction is from N50^0E to N280^0E while the dipping direction is from N20^0E to N355^0E. The maximum depth of each fault is from 1.5 to 3.6km deep. The Euler cross-section estimates the dipping and depths of faults along the Mersing fault zone which has not been estimated by previous researchers in this study area. This technique has proved that dipping, strike and depth of fault can be successfully determined by Euler Deconvolution technique as first introduced by Mushayandebvu *et al*. (2004) in the study of Great Dyke in Zimbabwe.

Table-1. Fault strikes, dipping, dipping direction and maximum depth below subsurface.

Fault	Dipping (^{0})	Strike	Estimate dipping direction	Max depth (km)
1	21.56	N 150^0 E	N 240^0 E	1.6
2	66.9	N 255^0 E	N 345^0 E	1.9
3	89	N 175^0 E	N 265^0 E	2.5
4	70.61	N 230^0 E	N 320^0 E	1.7
5	38.4	N 50^0 E	N 140^0 E	3.6
6	11.82	N 220^0 E	N 310^0 E	2.4
7	37.2	N 280^0 E	N 20^0 E	2.4
8	78.64	N 70^0 E	N 120^0 E	2.8
9	19.8	N 265^0 E	N 355^0 E	1.5
10	25.68	N 265^0 E	N 355^0 E	1.8

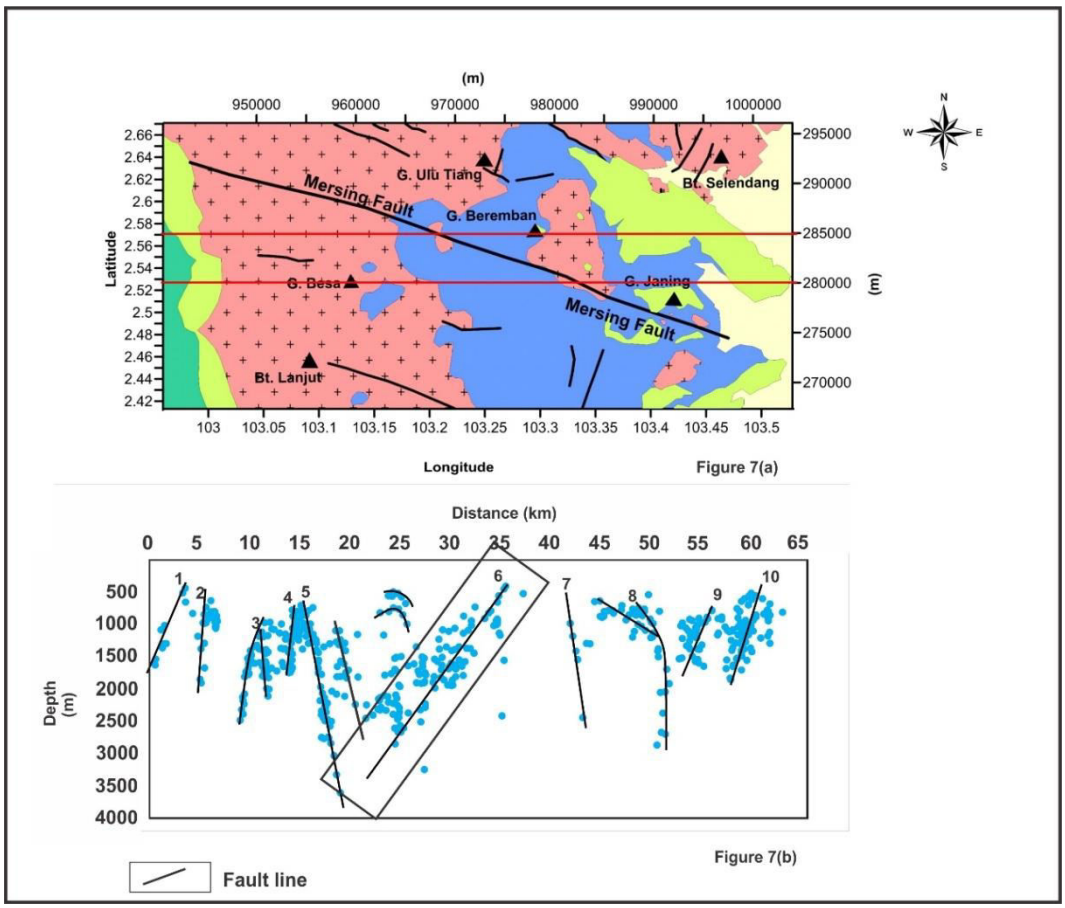

Figure-7(a). Geological map of Mersing fault with position of cross-section band.
Figure-7(b). Euler subsurface cross-section along the band.

CONCLUSIONS

Aeromagnetic data has successfully been processed to delineate Mersing fault zone which is trending N115^{0}E or along WNW-ESE in direction. The sense of its left lateral displacement was also detected in the magnetic anomaly RTE and filtered THD-TVD maps based on difference in magnetic susceptibility. By 3D Euler-Deconvolution applied on the aeromagnetic data, further discovered the point source of the Mersing fault and the minor faults surrounding it. Cross-section traverse along E-W of the Euler point source map proved the presence of fault within the upper crustal material at depth from 1.5 to 3km. Dips, dipping directions and strike of the faults were also characterized.

REFFERENCES

Agocs W.B., Paton J.R. 1966. Report on Airborne Magnetometer and Scintillation Counter Survey over part of Johore and Pahang (Area 4).

Amigun J.O., Afolabi O. and Ako B.D. 2012. Euler 3-D Deconvolution of Analytical Signal of Magnetic Anomalies over Iron Ore deposit in Okene, Nigeria. Jour. Emerging Trends Engg. Appld. Sci. (Jeteas). (4): 711-71.

Chong F.S., Cook R.H., Evans G.M. & Suntharalingam T. 1968. Geology and mineral resources of the Melaka-Mersing area. Geological Survey of Malaysia Annual Report. 89-94.

Cooper G.R.J. and Cowan D.R. 2008. Edge enhancement of potential-field data using normalized statistics, geophysics. 73(3): 1-4.

Cordell L. and V.J.S. Grauch. 1985. Mapping basement magnetization zones from aeromagnetic data in the San Juan basin, New Mexico, in W. J. Hinze, Ed.The utility of regional gravity and magnetic anomaly maps: SEG, 181-197.

El-Khafeef A.A and El Khodary S.T. 2011. Proprietary of Total Intensity Magnetic Data to Detect the Subsurface Structures and Tectonics of Southern Sinai Peninsula, Egypt. Journal of American Science. 7(3).

Gopal K.G. 2016. Interpretation of Gravity Data using 3D Euler Deconvolution, Tilt Angle, Horizontal Tilt Angle and Source Edge Approximation of the North-West Himalaya. Acta Geophysica. 64: 1112-1138.

Ghosh G.K and Dasgupta R. 2013. Edge Detection and Depth Estimation Using 3D Euler Deconvolution, Tilt angle derivatives and TDX derivatives using magnetic data of thrust fold belt area of Mizoram. 10th Biennial International Conference & Exposition.

Hutchison C.S., Tan D.N.K. 2009. Major Faults in Geology of Peninsular Malaysia. p. 267.

Mineral and Geoscience Department (MGD) Malaysia. 2014. Geological Map of Peninsular Malaysia. 9th Edition

Mushayandebvu M. F., V. Lesur, Reid A. B. and Fairhead J. D 2004. Grid Euler deconvolution with constraints for 2D structures. GEOPHYSICS. 69(2): 489-496.

Reid A. B., Allsop J. M., Granser H., Millett A. J. and Somerton I. W. 1990. Magnetic interpretation in three dimensions using Euler deconvolution: Geophysics. 55, 80-91.

Reid A.B. 1997. Euler Deconvolution, Past, Present and Future: A Review. In Proceedings of Exploration. 97: Fourth Decennial International Conference on Mineral Exploration edited by A. G. Gubins. pp. 861-864.

Reid A.B and Thurston J.B. 2014. The structural index in gravity and magnetic interpretation: Errors, uses, and abuses. Geophysics. 79(4): 61-66.

Samsudin Taib, Jamaluddin Othman & Noor Dalila Desa. 2000. The Magnetic Anomaly across Peninsular Malaysia between Muar and Endau. Geological Society of Malaysia Annual Geological Conference.

Stauffer, P.H., 1968. The Kuala Lumpur fault zone: a proposed major strike-slip fault across Malaya. Geol. Soc. Malaysia Newsletter, J 5, p. 2-4.

Syed Sheikh Almashoor. 1989. The role of Peninsular Malaysia's main range batholith in fault developments. Sains Malaysiana. 18(1): 3-11.

Thompson D.T. 1982. EULDPH: A new technique for making computer-assisted depth estimates from magnetic data, Geophysics. 47, 31-37.

Thurston J.B and Smith R.S. 1997. Automatic Conversation of Magnetic Data to Depth, Dip, and Susceptibility Contrast Using SPI™ Method. Geophysics. 62, 807-813.

Tjia H.D. 1972. Strike-slip faults in West Malaysia. 24th Internatiollal Geological Congress, Montreal, Canada, Section3 Tectonics. 255-262.

Tjia H.D. 1977. Western extension of the Kuala Lumpur fault zone. Geological Society of Malaysia Bulletin. 8, 123-125.